Article:
Tang, XH, Liu, JJ, Zhang, Y et al. (1 more author) (2018) Study on the influence of lysozyme crystallization conditions on crystal properties in crystallizers of varied sizes when temperature is the manipulated variable. Journal of Crystal Growth, 498. pp. 186-196. ISSN 0022-0248

https://doi.org/10.1016/j.jcrysgro.2018.06.023

Study on the Influence of Lysozyme Crystallization Conditions on Crystal Properties in Crystallizers of Varied Sizes When Temperature is the Manipulated Variable

Xi H. Tang[a], Jing J. Liu[b], Yang Zhang[a*] and Xue Z. Wang[a,b*]

[a] Engineering Centre for Pharmaceutical Engineering and Advanced Control, Guangdong Province, School of Chemistry and Chemical Engineering, South China University of Technology, Guangzhou, Guangdong, PR China, 510640

[b] School of Chemical and Process Engineering, University of Leeds, Leeds LS2 9JT, UK.

*** Correspondence authors:**

Professor Xue Z. Wang:

E-mail: xuezhongwang@scut.edu.cn Tel.: +86 (20) 87114000

Dr Yang Zhang

E-mail: ceyzhang@scut.edu.cn Tel: +86(20) 87114050

Abstract

In this work, crystallization experiments were conducted in three different sizes of crystallizers (5 and 100 ml, and 1 L) to study the influence of temperature on the crystallization of lysozyme. Lysozyme solutions with concentrations of 40 and 30 g L^{-1} and 10% (w/w) NaCl were used. The temperature was reduced from 20 to 0 °C with various cooling rate and stirring speed. The data indicated that crystallization with cooling but without agitation or with agitation but without cooling led to low yield and inconstancy between batches, whereas that with combined cooling and agitation resulted in tetragonal crystals with high yields. Parameters, including crystallization onset, crystal morphology, crystal size distribution, concentration, supersaturation, and yield were examined by in situ and ex situ observations. The observations within small cooling rate range of 0.030 - 0.111 °C min^{-1} indicated that minor changes in cooling rate could cause significant differences in these parameters. The comparison with thermostatic experiment showed that cooling could cause the crystal sizes to be widely dispersed. While high cooling rate lead shorter crystallization onset time and higher supersaturation, thereby result in larger crystal size, higher tendency of aggregation and wider crystal size distribution, low cooling rate can pose a great challenge to the temperature control in scale-up crystallization. The work also demonstrated that the crystallization conditions obtained from 5- and 100-ml crystallizers, from which well-defined crystals with high yields were obtained, could successfully be reproduced in 1-L crystallizer.

Keywords: A1. Protein crystallization; A2. Scale-up; A2. Cooling strategy; B1. Lysozyme; B3. Geometry similarity

1. Introduction

In small molecule pharmaceuticals, drugs containing active pharmaceutical ingredients (API) are often in crystalline form. Only small portion of over 240 biopharmaceutical products marketed in 2014[1] is in crystalline form. Strong evidences have demonstrated that delivery of drugs in crystalline form (rather than in liquids) has numerous advantages. The crystalline form of biopharmaceutical proteins not only has improved bioavailability and stability, but also adjustable solubility and easily controllable release [2]. In addition, compared to the liquid form, the crystalline form often has much longer shelf life, and is easier to handle, transport and store[3-5]. In order to produce crystals with the highest purity, crystallinity, and yield, it is important that the protein crystallization processes and conditions are optimized. Unoptimized operational conditions could lead to amorphous that have poor stability and low purity[3, 4, 6].

Large-scale production of protein crystals is highly challenging technically. The literatures on protein crystallization are largely about obtaining large single crystals suitable for X-Ray diffraction with the purpose of molecular structure analysis[7-12]. To obtain large single crystals suitable for X-ray diffraction, the crystallization is mainly carried out at a constant temperature in micro-crystallizers, which often is extremely time-consuming with relatively low yields[13]. Moreover, the preparative chromatographic method that are currently and widely used also involves rather cumbersome steps, as has mentioned by some researchers[14]: it is of low efficiency and hardly possible for operation at commercial scale production. However, in technical-scale protein crystallization processes, large single crystals are not essential[15]. Whilst the crystals can be relatively small, the growth rate should be high enough to meet the demands of industrial production and the requirements of GMP (Good Manufacturing Practices). Therefore, in contrast to the preparative chromatographic methods, the technical-scale crystallization may only focus on ensuring a low cost while maintaining high efficiency of purification[16].

Researches on scale-up of protein crystallization are still limited. Smejkal et

al.,[15] reported a study on crystallization of Canabiknmab Fab-Fragment and lysozymes under thermostatic conditions in three different reactor sizes. They found that successful crystallization scale-up, which was conducted thermostatically for 24 to 72 h, could be achieved when the maximum local energy dissipation is kept constant through different reactor sizes. The same method was applied to thermostatic crystallization of full-length antibodies and fragments in 1-L stirred tanks[17, 18]. Nevertheless, the isothermal crystallization is often time-consuming with low yield and reproducibility[16], as has demonstrated in the work of Smejkal et al.[15], in which the crystallization was conducted for 24 to 72 h. Hebel et al.,[19] studied the use of ionic liquids as additives in scale-up protein crystallization, and observed that the crystals had faster growth with higher yield. The introduction of an additive into crystallization is however controversial because it not only requires further edulcoration, but the remaining residues in the solvent channel may also have potential toxicity[18]. Similar observation has also been reported in solvent freeze-out method in protein crystallization, despite the encouraging results obtained from lysozyme purified from lysozyme-ovalbumin mixture, as reported by Diaz Borbon and Ulrich[20]. Maosoongnern et al.,[21] conducted seeded isothermal crystallization of lysozyme-ovalbumin mixture in a 100-ml vessel for 24 h and obtained comparable purification results with a yield of 80%. Protein crystallization based on gas diffusion has also been investigated[22-24]; it is however considerably difficult to control and difficult to achieve process scale-up.

Among parameters affecting the crystallization process, temperature can easily be controlled and implemented; it is therefore the preferred parameter chosen in controlling the supersaturation, given that the protein solubility in the solvent significantly varies with temperature. Manipulating temperature via cooling has been proven to be a better option in some protein crystallization studies[25-27], but the method is limited to μL-scale. Based on a study using a 15-μL crystallizer, Astier et al.,[25] summarized the advantages of temperature alteration as a crystallization parameter including constant composition, ease of control and monitoring and reversibility. Weber et al.,[26] successfully crystallized jack bean urease using the

extraction and cooling methods. The crystallization was carried out in the presence of three precipitants in a 50-ml non-agitated vessel for 2 days. The yield and purity were however low.

According to above, the influence of crystallization conditions, including cooling rate, stirring speed, concentration on product quality, and reactor sizes, as well as scalability and repeatability, should be systematically studied. The data obtained may add useful knowledge to the state of the art of protein crystallization. Therefore, in this work, we systematically studied the influence of cooling rates and stirring speed on the crystallization of lysozyme carried out in 5 ml, 100 ml and 1 L batch crystallizers. The morphology, size distribution and concentration of the crystals were characterized by an online imaging system, and the supersaturation profile was analyzed using an ex situ observation of sampling solutions.

2. Materials and Methods

2.1 Preparation of Samples and Crystallization Solutions

Hen egg white lysozyme powder used in the experiment was purchased from Sigma-Aldrich, Germany (No. 62971). In order to obtain tetragonal crystals, 0.1 M (mol of sodium acetate/ 1 L of water) sodium acetate buffer solution (titrated to pH = 4.5) was prepared. Lysozyme solutions were prepared by dissolving lysozyme powder (without further purification) in the buffer solution at final concentrations of 10 – 80 g L^{-1}. Precipitant solutions were prepared by dissolving sodium chloride pellet in the buffer solution at final concentrations of 3.5 – 25% (w/w). The concentration mentioned below refers to the concentration before mixing with the precipitant solution unless otherwise stated. Prior to use, the solutions were centrifuged at 1300 rpm for 15 min, filtered through 0.22 μm membrane filters, and stored at 20 ℃.

2.2 Parallel Crystallization Experiments

Parallel crystallization experiments were conducted in a sitting drop 24-well Linbro plate. Hen egg white lysozyme (HEWL) and NaCl solutions were mixed in the wells, and 25% (w/w) NaCl solution was placed in each cell as a dispersing agent. The plate was then sealed and incubated at a constant temperature of 20 ℃ in a constant humidity chamber for 24 h. After that, the samples were examined under a microscope.

2.3 Micro-batch Cooling Crystallization Experiments

For the micro-batch cooling crystallization experiments, feasible concentrations were screened in the above tests. Appropriate concentrations of HEWL and NaCl solutions were mixed to a final volume of 200 μL in a small transparent quartz crucible, which was then covered a clean slide to prevent evaporation. Subsequently, the crucible was placed in hot-stage reactor with high-precision controllable temperature and cooling rate. The investigated cooling rates were ranged from 0.03 – 1 ℃ min^{-1}. The temperature was reduced from 20 to 0 ℃ at controlled fixed cooling rates of 0.03 – 1 ℃ min^{-1}, thus the cooling duration was between 660 – 10 min. The entire cooling crystallization process was monitored and analyzed under a microscope, whereby the crystal sizes were measured and averaged.

2.4 Agitated Batch Cooling Crystallization

Three geometrically similar stirred tanks with working volumes of 5 ml, 100 ml and 1 L were used in the scale-up crystallization experiments. Flat-jacketed beakers were used as the reaction tanks, and anchor impellers were used for gentle mixing in the vessels. The ratio between heights and vessel filling heights was kept constant at one-third. Hen egg white lysozyme and NaCl solutions were mixed in the tanks, and a temperature probe, which was connected to the recirculation cooler to alter the

temperature, was then immersed in the solutions. The specialized temperature control software was used to control the cooling rates, which were fixed within the selected range. The stirring rate, determined by constant tip speed at different operating volumes, was set to a range of 50 – 250 rpm. The 2D Vision Probe purchased from Pharma Vision (Qingdao) Intelligent Technology Ltd. was used for real-time observation of the crystallization process. However, due to the excessive amount of crystals grown, the observation by 2D Vision Probe was carried out only to examine the crystallization onset, but not to determine the crystal's shapes and sizes. In the ex situ determination of crystal size distributions, a sample containing crystallization solution (as well as crystals) was withdrawn using a dropper at various time intervals and undergone two different processes as follows: (i) one part of the sample was placed under a microscope, specially equipped with a camera, thereby the crystal microscopic images were taken. The image frames were managed by 'SHAPE' software provided by Pharma Vision (Qingdao) Intelligent Technology Ltd. The software allows the processing of images, such as edge detection and particle identification, and the pre-processing and segmentation methods, such as contrast adjustment, noise removal, and multi-scale segmentation. After processing, the granule information, e.g. equivalent diameter, granule size distribution and aspect ratio, was exported; and (ii) the other part of the sample was filtered through a 0.22-μm syringe filter, and then diluted by 50 times prior to absorbance measurement at 280 nm by a UV spectrophotometer (UVmini-1240, SHIMADZU Company, Japan), from which its concentration was calculated. After the crystallization was completed, the bulk liquid was filtered through a sand core filter with a 0.22 μm membrane, and the filter cake was dried in a vacuum oven at 20 ℃ for 24 h. After sufficient amount of solid was obtained, e.g. samples obtained from 1 L scale, the crystal size distribution was measured by a Malvern Mastersizer 3000. Particle size determined by Mastersizer 3000 is based on laser diffraction, in which the intensity of laser light diffracted by sample is measured [the sample can be suspension, emulsion or dry powder]. After the obtained data is analyzed and the particle size distribution is calculated, the scattering pattern is created. The calculation method is based on sphere,

thus the obtained crystal size distribution is equivalent spherical volume distribution. In contrast, the crystal size distribution obtained by SHAPE software is count distribution. Consequently, crystal size distribution obtained from the two methods can be different.

3. Results and Discussion

3.1 Screening of Suitable Crystallization Conditions

The principle of crystallization screening has been described previously[28], and will not be detailed here. Figure 1 depicts various concentrations of lysozyme and sodium chloride (in % (w/w)). The crystallization drops were either described as 'clear drops' when no crystals were formed (Figure 2a) or tetragonal crystals (Figures 2b and 2c) and 'sea urchin' crystals (Figures 2d and 2e) when the crystals were formed. According to the literatures, the 'sea urchin' crystals have also been previously observed[29, 30]. Amorphous precipitates were not observed in our experiments.

Crystals were not observed in a mixture of 10 g L^{-1} lysozyme and 3.5% (w/w) NaCl (Figure 2a). In contrast, both tetragonal and 'sea urchin' crystals were observed in a mixture of 50 g L^{-1} lysozyme and 10% (w/w) NaCl (Figure 2d), while only 'sea urchin' crystals were formed in a mixture of 60 g L^{-1} lysozyme and 15% (w/w) NaCl. The results confirmed the computer-based simulation, which studied the influence of concentrations on protein crystallization, reported previously in the literature[31]. Tetragonal crystals were formed in a mixture of 30 g L^{-1} lysozyme and 6.5% (w/w) NaCl, and a mixture of 40 g L^{-1} lysozyme and 10% (w/w) NaCl; the crystal sizes in the former were larger than in the latter. The result suggests that a mixture of 30 or 40 g L^{-1} lysozyme and 10% (w/w) NaCl are the suitable initial conditions, thus were chosen in the study described in following sections. As illustrated in Figures 2b and 2c, it is worth noting that sizes of the tetragonal crystals varied with concentrations of lysozyme and NaCl concentration. Furthermore, in a mixture containing 50 g L^{-1} (or

60 g L^{-1}) lysozyme and 10% (w/w) NaCl, 'sea urchin' crystals surrounded by tetragonal crystals were observed (Figure 2d).

Figure 1

Figure 2

3.2 Effect of Cooling Rate on Non-agitated Micro-batch Crystallization of Lysozyme

To study the effect of cooling rate on non-agitated micro-batch crystallization of lysozyme, the crystallization of a mixture containing 30 g L^{-1} lysozyme and 10% (w/w) NaCl was carried out in a 200 μL micro-batch crystallizer. Linear cooling rates (from 0.03, 0.05, 0.1, 0.2, 0.3, … to 1.0 °C min^{-1} were investigated; at each cooling rate, the temperature was decreased from 20 to 0 °C. Crystal images were taken every 15 s throughout the crystallization. The data were presented in reference to the six images shown in Figure 3. Figure 3a shows an image of clear solution, taken before the start of the cooling; the image was used as a reference when analysing the images of slurries.

Figures 3b and 3c show the microscopic images (taken after the temperature reached 0 °C) of crystals grown at a cooling rate of 0.03 °C min^{-1} and 0.2 °C min^{-1}, respectively. The images illustrate that well-defined tetragonal crystals of lysozyme were produced, and neither amorphous precipitate nor 'sea urchin' crystals were formed. In addition, the number of crystals grown at a cooling rate of 0.2 °C min^{-1} was higher than that at a cooling rate of 0.03 °C min^{-1}. As described in the literature[32], it is possible that the degree of supersaturation at a cooling rate of 0.2 °C min^{-1} was higher compared with that at a cooling rate of 0.03 °C min^{-1}, thus the number of crystals was higher. The crystal size was around 15 μm in the former, whereas that was about 30 μm in the latter.

Figure 3d shows the image of crystals (taken when the temperature reached 0 °C) grown in batch crystallization at a cooling rate of 0.3 °C min^{-1}. The image unequivocally shows some large lysozyme crystals. Detailed comparison of Figure 3d

and Figure 3a (clear solution) indicated that the seeming background observed in Figure 3d were indeed very small particles. The same analysis was applied to the crystal image shown in Figure 3e, in which the crystals were grown at a cooling rate of 0.6 °C min^{-1}. A few large crystals were observed with very small particles in the background. Figure 3f shows that only small particles were formed when the cooling rate was 1.0 °C min^{-1}. It seems that nucleation occurred in Figures 3d and 3e in the areas far from the pre-existing large crystals. This was unlikely due to secondary nucleation, since secondary nucleation is often induced by contacts of crystals, fluid motion and so on[33-35]. Growing crystals with dislocations, defects or inclusions can also result in crack formation through the development of internal stresses and lead to the subsequent production of breakage fragments [36]. However, in the cases of Figure 3, there were no flows, no movement of crystals and less shear force in the stagnant systems. And more importantly, the fine particles were not formed around the large crystals but many were formed very far from the pre-existing crystals. We reckon that the fine particles in the background of Figure 3d were due to spontaneous primary nucleation. These results indicate that well-defined lysozyme crystals preferably grow at a cooling rate range of 0.03 to 0.2 °C min^{-1}. Such cooling rates are considered very low, which can be a challenge in large-scale crystallization. Low cooling rates could however contribute to more suitable kinetics, mass transfer rate or molecular diffusion rate. Essentially, this could also be the reason why some protein crystallizations take time (i.e. days or as long as weeks) to reach equilibrium.

Figure 3

3.3 Effect of Agitation and Cooling on Crystallization of Lysozyme

Lysozyme was crystallized in an up-scale 5-ml agitated crystallizer at the optimal cooling rates (0.030 - 0.2 °C min^{-1}) obtained in section 3.2. The experiments were designed to examine the influence of cooling (with and without cooling) and agitation (with and without agitation) on crystallization of lysozyme. Four crystallization conditions (denoted as (a), (b), (c) and (d)) are summarized in Table 1. And to

determine the reproducibility, four batch crystallizations were conducted under each condition; thus a total of sixteen experiments were conducted. Each of the twelve batches conducted under conditions (a), (b) and (d) with cooling had a batch time of (20 ℃ – 0 ℃)/0.048(℃ min-1) = 417 min. Similarly, each of the four batches conducted under condition (c) without cooling also had a batch time of 417 min.

Figure 4 illustrates a plot of yields from sixteen experiments conducted under four conditions. As demonstrated in Figure 4, high yields were achieved from eight batches conducted under conditions (a) and (b) with cooling and agitation, and about 92.5% yield was obtained from four batches conducted under condition (a) with initial lysozyme concentration of 40 g L^{-1}; and around 89% yield was obtained from four batches conducted under condition (c) with initial lysozyme concentration of 30 g L^{-1}. In contrast, only about 45% to 70% yields were obtained from eight batches carried out under conditions (c) and (d), without cooling or without agitation. Thus, it can be concluded that at a given batch time, high yield can be achieved by the combination of cooling and agitation. Furthermore, observation from Figure 4 shows that batches with combined cooling and agitation had high repeatability, while those with cooling but without agitation or with agitation but without cooling had poor repeatability.

As has mentioned in previous study, crystal growth is controlled by mass transfer or molecular diffusion[15]; therefore, good agitation/mixing increases mass and heat transfer rates. Smejkal et al., have also stressed the importance of agitation.

Figure 4

3.4 In situ and Ex situ Observation of Agitated Batch Crystallization of Lysozyme

Online imaging has been proven to be a useful tool for monitoring the crystallization process[37-40]. Figure 5 displays the online images of crystallization drop containing 40 g L^{-1} lysozyme and 10% (w/w) NaCl. The crystallization was carried out in a 5-ml crystallizer, at cooling rate of 0.048 ℃ min^{-1} (at which the temperature was decreased from 20 ℃ to 0 ℃) with an agitation speed of 210 rpm. As shown in Figures 5a and 5b, within 2 min after lysozyme and NaCl were mixed,

very small particles were appeared. This is particularly common in lysozyme crystallization: when lysozyme is mixed with NaCl, local supersaturation can be so high that it causes nucleation, and at this point, the concentration of these very small particles remained relatively low. As illustrated in Figures 5b and 5c, these small particles continuously grew during the following 40 min. They, however, remained too small that could not be collected in the sampling or by filtering through 0.22-μm membrane. After about 46 min, the crystals began to grow more rapidly (Figures 5c and 5d) and the particle concentration sharply increased (Figures 5d - 5e), indicating that crystal nucleation has been taken place. Nonetheless, because the crystal nucleation has in fact occurred (within 2 min after lysozyme and NaCl were mixed) prior, we consider this stage as 'crystallization onset' . In this stage, it is difficult to determine whether primary or secondary nucleation or even both occurred. However, primary nucleation was more likely to dominate due to relatively lower crystal concentration prior (low collision possibility) and sufficiently high supersaturation (secondary nucleation generally occurs at a lower supersaturation[33]). After that, the particle concentration was too high (Figure 5f) that the 2D vision probe was not able to monitor the subsequent crystal growth process. Thus, in this work, the online imaging was only used to examine crystals during 'crystallization onset' (but not during crystal growth).

We therefore carried out a so-called ex situ observation to monitor the changes of crystal size and morphology. Figure 6 displays the crystal images at 50, 180, 420 and 660 min. The samples were taken at various temperatures, 17.6, 11.4, 0 ℃ and 0 ℃ held for 240 min. The images indicate that small crystals without aggregates were observed during the 'crystallization onset' (Figure 6a). Additionally, continuous cooling caused the increasing number and size of tetragonal crystals, as well as aggregates (Figure 6b). After 420 min (at 0 ℃), the number and size of crystals were further increased (Figure 6c); however, the number of small crystals (sizes of < 10 μm) was still high, which indicated that new nuclei were formed at this stage. After 240 min at 0 ℃ (Figure 6d), the number of large crystals (sizes of > 30 μm) increased; and similarly, the number of small crystals significantly increased. This observation

indicated that nucleation continuously took place throughout the crystallization process, thus the crystal sizes were largely dispersed. Tait et al. [41] found that secondary nucleation of lysozyme crystallization is significantly affected by attrition. Thus it is possible that when the above-mentioned primary nucleation and crystal growth consumed the supersaturation to a lower level and increased the crystal concentration, secondary nucleation was induced. During the entire crystallization process, one crystal form, tetragonal crystal, was observed. Overall, it appears that new crystals, which were continuously nucleated during crystal growth stage, and tendency of aggregation led to the broadening of crystal size distribution. This allowed us to investigate the effect of cooling on lysozyme crystallization; however, intuitive comparisons with the crystal size distributions measured using SHAPE software are discussed in section 3.5.

Figure 5

Figure 6

3.5 Effect of Cooling Rate on 5-ml Agitated Batch Crystallization of Lysozyme

We further examined the effect of the optimal cooling rate (0.03 – 0.2 °C min^{-1}) on the crystallization of lysozyme in a 5-ml crystallizer. The crystallization conditions were as follows: mixture, 40 g L^{-1} lysozyme, 10% (w/w) NaCl and 0.1 M sodium acetate buffer, pH 4.5; stirring speed, 210 rpm; temperatures, continuous decrease from 20 to 0 °C; cooling rates, 0.111, 0.048 and 0.030 °C min^{-1}; cooling times, 180, 420 and 660 min. After the temperature was decreased to 0 °C at cooling rates of 0.111 and 0.048 °C min^{-1}, it was then kept at 0 °C until the total time reached 660 min. In thermostatic experiment (control), the temperature was also maintained at 20 °C for 660 min, in which the cooling rate was considered to be 0 °C min^{-1}. Figure 7 shows the crystallization onset determined by online imaging. The microscopic images of lysozyme crystals (at 660 min) obtained at cooling rates of 0.111, 0.048, 0.030 and 0 °C min^{-1} are shown in Figure 8, and the changes in crystal size distributions at different

time intervals are shown in Figure 9.

Figure 7

Figure 8

Figure 9

These results indicated that lysozyme underwent the crystallization process following the results presented in Figure 5, irrespective of crystallization conditions. However, the crystallization onset time (Figure 7), the degree of aggregation (Figure 8) and crystal size distribution (Figure 9) were different at different cooling rates. Specifically, as demonstrated in Figure 7, the crystallization onset time (and the corresponding error) decreased with increasing cooling rate. The crystallization onset time at a cooling rate of 0.03 °C min^{-1} was nearly half of the thermostatic experiment. It appears that high cooling rate causes high supersaturation; as a result, the nucleation was induced during the early stage of the crystallization[33, 42]. Moreover, because the rate of nucleation is high at high supersaturation (or the rate of nucleation is low at low supersaturation) while the stirring rate is fixed[41, 42], the particle concentration changed more quickly, thus the crystals were more readily observed.

Tetragonal crystals and crystal clusters were obtained in all batches. As demonstrated in Figure 8, when the cooling rate was increased, the average sizes of crystals were larger and the aggregation of crystals became more apparent, and the proportions of the large and small crystals seemed to be higher. This may be due to higher supersaturation, which promotes more rapid crystal growth[31], while more nucleation continues to be induced (similarly to Figure 6). In addition, the increasing number of large and small crystals also increases the probability of collision and attrition between these crystals, which eventually leads to secondary nucleation[41] and aggregation.

It can be inferred from the results shown in Figure 9 that the cooling process causes the crystal size distribution to be gradually widened. At a high cooling rate of 0.111 °C min^{-1} with short crystallization onset time, the crystals formed prior to the crystallization onset were relatively small. Because higher supersaturation leads to higher nucleation rate[33], larger numbers of crystals were nucleated within such

short period of time. Thus, the size distribution measured within the crystallization onset time was narrower than that observed in other experiments. Subsequently, crystallization onset was reached and nucleation occurred. As mentioned earlier, high supersaturation leads to rapid crystal growth and aggregation, while continuously formed new nuclei and increased the crystal concentration; this could lead to wider size distribution (Figure 9a). Meanwhile, from the empirical power law expressions of nucleation rate, it is proportional to the stirring speed, crystal concentration and supersaturation[43]. Thus, with both higher crystal concentration and supersaturation, the nucleation rate was higher which also made the distribution wider. On the contrary, at a low cooling rate of 0.030 °C min^{-1}, the crystals grew more slowly due to a longer crystallization onset time, their sizes thus were relatively larger. In addition, since the supersaturation was lower at this cooling rate, fewer numbers of crystals were nucleated at the early stage of crystallization; as a result, the crystal size distribution during the crystallization onset was wider (Figure 9c). For the thermostatic experiment, the supersaturation that was more gradually and slowly consumed due to no cooling caused the crystals to grow more slowly almost without further nucleation after the crystallization onset. Therefore, the width of its crystal size distribution for the thermostatic experiment was nearly unchanged (Figure 9d) and assembled those grown at slow cooling rate (Figure 9c). These findings demonstrate that high cooling rate causes shorter crystallization onset time, larger average crystal sizes and wider crystal size distribution. It is generally accepted that maintaining the temperature (after the cooling was completed) for extended period of time can result in the dissolution of small crystals, while promote growth of larger crystals, thereby lead to narrower crystal size distribution. This, however, contrasts with the results observed in the present work (Figures 9a and 9b). To validate such potential error, which may be caused by the measuring or sampling method, the particle size distribution was further examined using the Malvern method, which is discussed in section 3.6.

The ex situ sampling method was adopted to determine the concentration and the supersaturation profiles of the crystallization process in a larger crystallizer (100 ml).

Similarly to that in 5-ml crystallizer, cooling rates of 0.111，0.048，0.030 ℃ min^{-1} were used for the crystallization in 100-ml crystallizer. Additionally, all other conditions were the same except for stirrer speed. According to the scale-up rule of constant impeller tip speed as well as, the stirrer speed in 100-ml crystallizer was adjusted to 100 rpm (compared with 210 rpm in 5-ml crystallizer). In addition, a study, which conducted isothermal crystallization of lysozyme and lipase in water-soluble substituted alkyl ammonium-based ionic liquids, has reported that the influence of agitation rate on crystallization kinetics can be neglected when the stirring speed is maintained between 100 to 300 rpm[19]. At certain time interval, the crystallization solution was sampled and then diluted by 50 times. After that, its UV absorbance at 280 nm was measured, and the lysozyme concentration curves were obtained.

The solubility data of HEWL has been previously obtained and fitted by Lin et al.[42]. The empirical equation of lysozyme solubility (10% (w/w) NaCl) can be expressed as follows:

$$lnC_s = 7.827 - 8339.738/T + 3.959lnT \quad (1)$$

Where Cs is the solubility of HEWL in mg of HEWL/ml of solvent and T is the temperature. Using the concentration measured off-line and the solubility, the supersaturation was calculated as follows:

$$\beta = (C_i - C_s)/C_s \quad (2)$$

Where β is the supersaturation (dimensionless) and C_i is the immediate concentration of lysozyme in solution. Figure 10 shows the crystallization onset time measured by online imaging in 100-ml crystallizer, and Figure 11 shows the changes in crystal size distributions of the crystallization solutions sampled at different time intervals. The changes of lysozyme concentration and supersaturation in the sampled solutions are shown in Figure 12.

Figure 10

Figure 11

Figure 12

The results obtained from the 100-ml crystallizer were comparable to those

obtained from the 5-ml crystallizer. Tetragonal crystals and crystal clusters were observed in all batches (data not shown). At slower cooling rate, the crystallization onset times were prolonged (with larger error between each batch) (Figure 10) and the crystal size distributions were similar to those of the thermostatic experiment (Figures 11c and 11d). At higher cooling rate, the crystal size distribution during the crystallization onset was narrower, while later became wider (Figure 11).

As shown in Figure 12a, prior to the crystallization onset, the solution concentrations slowly decreased. This may be due to nucleation and growth of small crystals (similar to Figures 5b and 5c), which consume small amount of solution lysozyme. As anticipated, when the crystallization progressed to the crystallization onset, the concentration of solution lysozyme was instantaneously dropped. However, when the temperature was dropped to 0 °C, the solution concentration in each batch was similar. Yields, measured when the temperature reached 0 °C, of about 91% were obtained from all cooling rates (> 0 °C min^{-1}). Therefore, comparison of sizes of the crystals obtained at different cooling rates can be meaningful. At a high cooling rate of 0.111 °C min^{-1} and after the 0 °C temperature was maintained for 240 min (or at a total of 420 min), the yield increased to 94%. At a cooling rate of 0.048 °C min^{-1} and after the 0 °C temperature was maintained for 240 min (or at a total of 660 min), the yield increased to only 92%. The observation indicates that at slower cooling rate, longer temperature holding time may be required to achieve higher yield.

To verify the statement about supersaturation mentioned above, the supersaturation profiles were obtained and analyzed. As illustrated in Figure 12b, which shows the supersaturation profile of each batch, the supersaturation β rapidly increased (after the cooling process was started) and reached a turning point, where β was sharply drop. The turning point indicates nucleation, while the total time required to reach such point (from when the cooling process was started) is the crystallization onset time. The results indicated that the higher the cooling rate, the shorter the crystallization onset time and the higher the β value at nucleation point. The observation was consistent with theoretical analysis: high cooling rate leads to high supersaturation (prior nucleation) and short crystallization onset. Although a few

crystals are formed prior to the crystallization onset, higher β value at nucleation point can result in higher number of nuclei; thus, the crystal size distribution is narrower. This explanation aligns with the results displayed in Figure 11, which shows that the crystal size distribution at the crystallization onset is narrower at higher cooling rate. At highest cooling rate of 0.111 °C min^{-1}, the highest supersaturation, which was maintained at over 1.0 for 300 min, promoted rapid primary nucleation and crystal growth while continuously induced secondary nucleation. As a result, the numbers of both small and large crystals as well as the degree of aggregation increased, causing the crystal size distribution to be the broadest. Furthermore, at about 180 min, the supersaturation was largely fluctuated. According to the literature[31], the upward trend may be due to crystals that are grown at inappropriate rates (insufficiently consume supersaturation), whereas the downward trend may be caused by secondary nucleation. Compared with a cooling rate of 0.048 °C min^{-1}, the supersaturation was lower at 0.030 °C min^{-1}, thus the nucleation rate and crystal growth rate were lower. In addition, similar fluctuation was also observed between 180 to 300 min. However, the cooling rate of 0.030 °C min^{-1} had lower supersaturation at the nucleation point, thus fewer numbers of crystals were nucleated and the crystal size distribution was relatively narrower. As a result, the crystal size distributions shown in Figures 11c and 11d were similar.

3.6 Crystallization of Lysozyme in 1-L Crystallizer

As mentioned earlier, in small molecular crystallization, maintaining the temperature for extended period of time can lead to the dissolution of small crystals and the promotion of growth of larger crystals; and as a result, the crystal size distribution became narrower. This is in contrast with lysozyme system. To validate potential errors, which may be caused by the measuring or sampling method, Malvern method was used to further determine the crystal size distribution. Because measurement in Malvern method requires larger sample volume, the crystallization was carried in a larger crystallizer (1 L) that have similar geometrical set-up to other

smaller crystallizers, and the same crystallization conditions was applied. Initial crystallization solution contained 40 g L^{-1} lysozyme, 10% (w/w) NaCl and 0.1 M sodium acetate buffer, pH 4.5. The stirrer speed, estimated according to the scale up rule of constant impeller tip speed, was set at 50 rpm. The temperature was decreased from 20 to 0 ℃ at a cooling rate of 0.048 ℃ min^{-1}. After the temperature reached 0 ℃, the stirrer speed was adjusted to 50 rpm, and the 0 ℃ temperature was maintained for additional 240 min. The solutions were sampled for analysis at total times of 540 min, 600 (540+60) min and 660 (540+120) min.

Well-defined tetragonal crystals with a yield of 91.7% were obtained after the temperature reached 0 ℃ (at a total time of 420 min). The yield was increased by 0.4% after the 0 ℃ temperature was maintained for 240 min. This minor increase of yield (from a total time of 420 min to 660 min) was consistent with the nearly invisible changes of solution concentration and supersaturation (Figure 12, solid squares).

Figure 13 shows the size distributions of crystals sampled at 540, 600 and 660 min. The proportions of small crystals increased from 540 min to 600 min and to 660 min while those of medium size decreased (Figure 13, arrows). It is however not fully understood what caused these changes and whether or not these changes are of significance. According to a study by Dai et al.,[44] which reported that at appropriate NaCl concentration, large aggregates formed in the lysozyme solution could be disaggregated. As shown in Figure 6d, clear aggregates of large and small crystals were observed. Thus, the observation in Figure 13 could be due to the disaggregation of the crystals that were aggregated when the temperature was hold at 0 ℃.

Figure 13

4. Conclusions

In the crystallization of solution containing 40 g L^{-1} lysozyme and 10% (w/w) NaCl in non-agitated micro-batch crystallizer, the optimal (slow) cooling rates of 0.03 to 0.2 ℃ min^{-1} resulted in crystals with proper morphology and size distribution. At a higher cooling rate, spontaneous primary nucleation seemed to occur for the second time and led to the formation of very fine particles in large numbers. The effect of such optimal

cooling rate was investigated in 5- and 100-ml, and 1-L agitated crystallizer. The results showed that crystallization with combined cooling and agitation resulted in suitable crystals with high yield, and the entire crystallization was completed within a considerably short time. In contrast, crystallization with cooling but without agitation or crystallization with agitation but without cooling could lead to poor repeatability and low yield. The in situ observation and the determination of crystallization onset were conducted using online imaging. The ex situ observation, in which solutions were sampled from crystallization mixture, was also adopted to examine the changes in crystal morphology, size distribution, concentration, supersaturation and yield. The data indicated that the cooling process in crystallization could cause the crystal size distribution to be wider. While higher cooling rate could lead to shorter crystallization onset time, larger crystal size, larger amount of aggregation and wider crystal size distribution, lower cooling rate resulted in crystals that assembled those of thermostatic experiment. This work demonstrates that temperature is an important factor in the success of protein crystallization process. This can be particularly challenging in some scale-up crystallizations, whose temperature is difficult to control. Furthermore, in contrast to small molecular crystallization, when the system was cooled down to the set temperature and maintained for a certain period of time, the crystal size distribution was not becoming narrower. Lastly, the future work may focus on the validation of experiments and the explanation of phenomena observed in this work.

Acknowledgements

This work was financially supported by the National Natural Science Foundation of China (NNSFC) (grant references: 91434126 and 61633006), the Natural Science Foundation of Guangdong Province (grant reference: 2014A030313228), the Guangdong Provincial Science and Technology Projects under the Scheme of Applied Science and Technology Research Special Funds (grant reference: 2015B020232007), as well as the pharmaceutical company whose name cannot be disclosed due to confidentiality agreement. The authors would like to extend their thanks to Dr Jianguo Cao of Pharmavision (Qingdao) Intelligent Technology Limited (www.pharmavision-ltd.com) who provided assistance in the imaging and the ATR FTIR instrument. The authors would also like to thank the anonymous reviewers for their critically reading the manuscript and valuable comments.

References

[1] G. Walsh, Biopharmaceuticals benchmarks, Nat. Biotechnol. , 32 (2014) 992–1000.

[2] S.K. Basu, C.P. Govardhan, C.W. Jung, A.L. Margolin, Protein crystals for the delivery of biopharmaceuticals, Expert Opin. Biol. Th., 4 (2004) 301-317.

[3] J. Drenth, C. Haas, Protein crystals and their stability, J. Cryst. Growth, 122 (1992) 107-109.

[4] A.A. Elkordy, R.T. Forbes, B.W. Barry, Stability of crystallised and spray-dried lysozyme, Int. J. Pharm. , 278 (2004) 209-219.

[5] M.X. Yang, B. Shenoy, M. Disttler, R. Patel, M. McGrath, S. Pechenov, A.L. Margolin, Crystalline monoclonal antibodies for subcutaneous delivery, PNAS 100 (2003) 6934-6939.

[6] B. Shenoy, Y. Wang, W.Z. Shan, A.L. Margolin, Stability of crystalline proteins, Biotechnol. Bioeng. , 73 (2001) 358-369.

[7] H. Hou, Y. Liu, B. Wang, F. Jiang, H.R. Tao, S.Y. Hu, D.C. Yin, Recrystallization: a method to improve the quality of protein crystals, J. Appl. Crystallogr. , 48 (2015) 758-762.

[8] S. Maki, Y. Oda, M. Ataka, High-quality crystallization of lysozyme by magneto-Archimedes levitation in a superconducting magnet, J. Cryst. Growth, 261 (2004) 557-565.

[9] I. Yoshizaki, T. Sato, N. Igarashi, M. Natsuisaka, N. Tanaka, H. Komatsu, S. Yoda, Systematic analysis of supersaturation and lysozyme crystal quality, Acta Crystallogr., Sect D: Biol. Crystallogr. , 57 (2001) 1621-1629.

[10] H. Koizumi, S. Uda, K. Tsukamoto, M. Tachibana, K. Kojima, J. Okada, J. Nozawa, Crystallization Technique of High-Quality Protein Crystals Controlling Surface Free Energy, Cryst. Growth Des., 17 (2017) 6712-6718.

[11] A. Adawy, E. Rebuffet, S. Tornroth-Horsefield, W.J. de Grip, W.J.P. van Enckevort, E. Vlieg, High Resolution Protein Crystals Using an Efficient Convection-Free Geometry, Cryst. Growth Des., 13 (2013) 775-781.

[12] J.D. Ng, J.K. Baird, L. Coates, J.M. Garcia-Ruiz, T.A. Hodge, S.J. Huang, Large-volume protein crystal growth for neutron macromolecular crystallography, Acta Cryst. F, 71 (2015) 358-370.

[13] R. Giege, A historical perspective on protein crystallization from 1840 to the present day, FEBS J., 280 (2013) 6456-6497.

[14] J. Thömmes, M. Etzel, Alternatives to Chromatographic Separations, Biotechnol. Progr. , 23 (2007) 42-45.

[15] B. Smejkal, B. Helk, J.M. Rondeau, S. Anton, A. Wilke, P. Scheyerer, J. Fries, D. Hekmat, D. Weuster-Botz, Protein crystallization in stirred systemsscale-up via

the maximum local energy dissipation, Biotechnol. Bioeng. , 110 (2013) 1956-1963.

[16] S. Schmidt, D. Havekost, K. Kaiser, J. Kauling, H.K. Henzler, Crystallization for the downstream processing of proteins, Eng. Life Sci., 5 (2005) 273-276.

[17] B. Smejkal, N.J. Agrawal, B. Helk, H. Schulz, M. Giffard, M. Mechelke, F. Ortner, P. Heckmeier, B.L. Trout, D. Hekmat, Fast and scalable purification of a therapeutic full-length antibody based on process crystallization, Biotechnol. Bioeng. , 110 (2013) 2452-2461.

[18] D. Hebel, S. Huber, B. Stanislawski, D. Hekmat, Stirred batch crystallization of a therapeutic antibody fragment, J. Biotechnol. , 166 (2013) 206-211.

[19] D. Hebel, M. Ürdingen, D. Hekmat, D. Weusterbotz, Development and Scale up of High-Yield Crystallization Processes of Lysozyme and Lipase Using Additives, Cryst. Growth Des., 13 (2013) 2499-2506.

[20] V.D. Borbon, J. Ulrich, Solvent freeze out crystallization of lysozyme from a lysozyme-ovalbumin mixture, Cryst. Res. Technol. , 47 (2012) 541-547.

[21] S. Maosoongnern, C. Flood, A.E. Flood, J. Ulrich, Crystallization of lysozyme from lysozyme - ovalbumin mixtures: Separation potential and crystal growth kinetics, J. Cryst. Growth, 469 (2017) 2-7.

[22] N.E. Chayen, Comparative studies of protein crystallization by vapour-diffusion and microbatch techniques, Acta Crystallogr., Sect D: Biol. Crystallogr. , 54 (1998) 8-15.

[23] M.B. Gross, M. Kind, Comparative Study on Seeded and Unseeded Bulk Evaporative Batch Crystallization of Tetragonal Lysozyme, Cryst. Growth Des., 17 (2017) 3491-3501.

[24] U.V. Shah, N.H. Jahn, S.S. Huang, Z.Q. Yang, D.R. Williams, J.Y.Y. Heng, Crystallisation via novel 3D nanotemplates as a tool for protein purification and bio-separation, J. Cryst. Growth, 469 (2017) 42-47.

[25] J.-P. Astier, S. Veesler, Using Temperature To Crystaltize Proteins: A Mini-Review, Cryst. Growth Des., 8 (2008) 4215-4219.

[26] M. Weber, M.J. Jones, J. Ulrich, Crystallization as a Purification Method for Jack Bean Urease: On the Suitability of Poly(Ethylene Glycol), Li2SO4, and NaCl as Precipitants, Cryst. Growth Des., 8 (2008) 711-716.

[27] J.J. Liu, C.Y. Ma, X.Z. Wang, Imaging protein crystal growth behaviour in batch cooling crystallisation, Chin. J. Chem. Eng. , 24 (2016) 101-108.

[28] D. Hekmat, D. Hebel, H. Schmid, D. Weuster-Botz, Crystallization of lysozyme: From vapor diffusion experiments to batch crystallization in agitated ml-scale vessels, Process Biochem. , 42 (2007) 1649-1654.

[29] M. Muschol, F. Rosenberger, Liquid-liquid phase separation in supersaturated lysozyme solutions and associated precipitate formation/crystallization, J. Chem. Phys. , 107 (1997) 1953-1962.

[30] O. Galkin, P.G. Vekilov, Are nucleation kinetics of protein crystals similar to those of liquid droplets?, J. Am. Chem. Soc. , 122 (2000) 156-163.

[31] J.J. Liu, Y.D. Hu, X.Z. Wang, Optimization and control of crystal shape and size in protein crystallization process, Comput. Chem. Eng. , 57 (2013) 133-140.

[32] M.W. Burke, R. Leardi, R.A. Judge, M.L. Pusey, Quantifying main trends in lysozyme nucleation: The effect of precipitant concentration, supersaturation, and impurities, Cryst. Growth Des., 1 (2001) 333-337.

[33] J.W. Mullin, Crystallization (Fourth Edition), fourth ed., Butterworth-Heinemann, Oxford, 2001.

[34] S.G. Agrawal, A.H.J. Paterson, Secondary Nucleation: Mechanisms and Models, Chem. Eng. Commun. , 202 (2015) 698-706.

[35] G.D. Botsaris, Secondary Nucleation — A Review, in: J.W. Mullin (Ed.) Industrial Crystallization, Springer US, Boston, MA, 1976, pp. 3-22.

[36] A.A. Chernov, N.P. Zaitseva, L.N. Rashkovich, Secondary nucleation induced by the cracking of a growing crystal: KH2PO4 (KDP) and K(H,D)2PO4 (DKDP), J. Cryst. Growth, 102 (1990) 793-800.

[37] Z.K. Nagy, G. Fevotte, H. Kramer, L.L. Simon, Recent advances in the monitoring, modelling and control of crystallization systems, Chem. Eng. Res. Des., 91 (2013) 1903-1922.

[38] L.L. Simon, H. Pataki, G. Marosi, F. Meemken, K. Hungerbuhler, A. Baiker, S. Tummala, B. Glennon, M. Kuentz, G. Steele, H.J.M. Kramer, J.W. Rydzak, Z.P. Chen, J. Morris, F. Kjell, R. Singh, R. Gani, K.V. Gernaey, M. Louhi-Kultanen, J. O'Reilly, N. Sandler, O. Antikainen, J. Yliruusi, P. Frohberg, J. Ulrich, R.D. Braatz, T. Leyssens, M. von Stosch, R. Oliveira, R.B.H. Tan, H.Q. Wu, M. Khan, D. O'Grady, A. Pandey, R. Westra, E. Delle-Case, D. Pape, D. Angelosante, Y. Maret, O. Steiger, M. Lenner, K. Abbou-Oucherif, Z.K. Nagy, J.D. Litster, V.K. Kamaraju, M.S. Chiu, Assessment of Recent Process Analytical Technology (PAT) Trends: A Multiauthor Review, Org. Process Res. Dev. , 19 (2015) 3-62.

[39] A.J. Malkin, Y.G. Kuznetsov, A. McPherson, In situ atomic force microscopy studies of surface morphology, growth kinetics, defect structure and dissolution in macromolecular crystallization, J. Cryst. Growth, 196 (1999) 471-488.

[40] G. Sazaki, A.E.S. Van Driessche, G.L. Dai, M. Okada, T. Matsui, F. Otalora, K. Tsukamoto, K. Nakajima, In Situ Observation of Elementary Growth Processes of Protein Crystals by Advanced Optical Microscopy, Protein Peptide Lett., 19 (2012) 743-760.

[41] S. Tait, E.T. White, J.D. Litster, A Study on Nucleation for Protein Crystallization in Mixed Vessels, Cryst. Growth Des., 9 (2009) 2198-2206.

[42] C. Lin, Y. Zhang, J.J. Liu, X.Z. Wang, Study on nucleation kinetics of lysozyme crystallization, J. Cryst. Growth, 469 (2017) 59-64.

[43] J. Garside, Industrial crystallization from solution, Chem. Eng. Sci., 40 (1985)

1 3-26.
2 [44] G.L. Dai, W.R. Hu, Effect of NaCl on Liquid/Liquid Diffusion Lysozyme Crystal
3 Growth, Acta Chim. Sinica 61 (2003) 520-525.
4
5

Table 1 Crystallization conditions in 5-ml crystallizer*

Batch number	Initial lysozyme concentration, g L^{-1}	Cooling rate, °C min^{-1}	Stirrer speed, rpm
(a)	40	0.048	210
(b)	30	0.048	210
(c)	40	No cooling, constant T	210
(d)	30	0.048	No agitation

*Mixture of 10% (w/w) NaCl and 0.1 M sodium acetate buffer, pH 4.5 was used; the temperature was reduced from 20 to 0 °C.

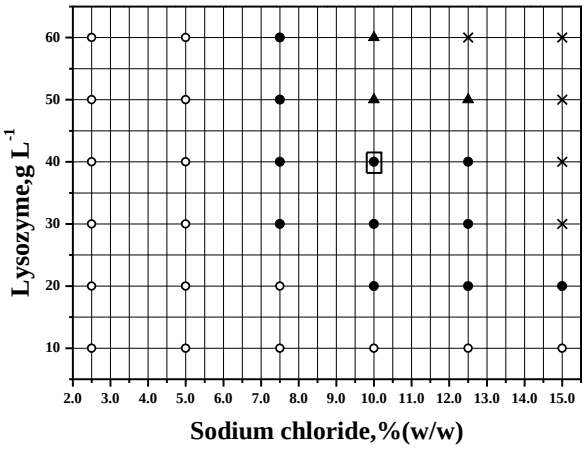

Figure 1: Phase diagram of lysozyme obtained from parallel experiments carried out at 20 °C using 0.1 M sodium acetate buffer, pH 4.5. Open circles, clear drop; solid circles, tetragonal crystals were formed; triangle, both tetragonal and "sea urchin" crystals were formed; and crosses, "sea urchin" crystals were formed. The square represents the initial concentrations of lysozyme and NaCl selected for subsequent experiments.

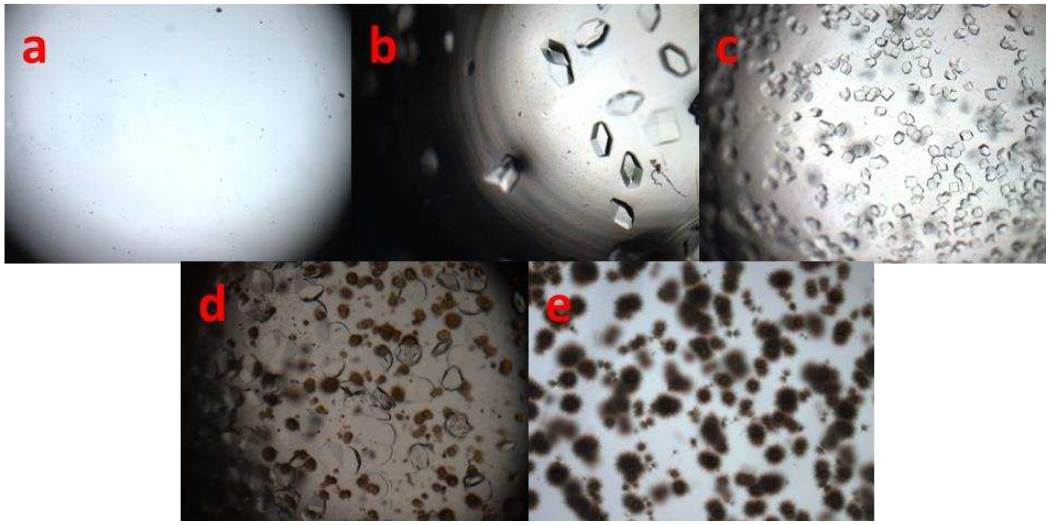

Figure 2: Microscopic images of crystals obtained from various lysozyme and NaCl concentrations: (a) clear drop obtained from 10 g L^{-1} lysozyme and 3.5% (w/w) NaCl; (b) small

number of tetragonal crystals with large sizes obtained from 30 g L^{-1} lysozyme and 6.5% (w/w) NaCl; (c) large number of tetragonal crystals with small sizes obtained from 40 g L^{-1} lysozyme and 10% (w/w) NaCl; (d) both tetragonal and "sea urchin" crystals obtained from 50 g L^{-1} lysozyme and 10% (w/w) NaCl; and (e) "sea urchin" crystals obtained from 60 g L^{-1} lysozyme and 15% (w/w) NaCl.

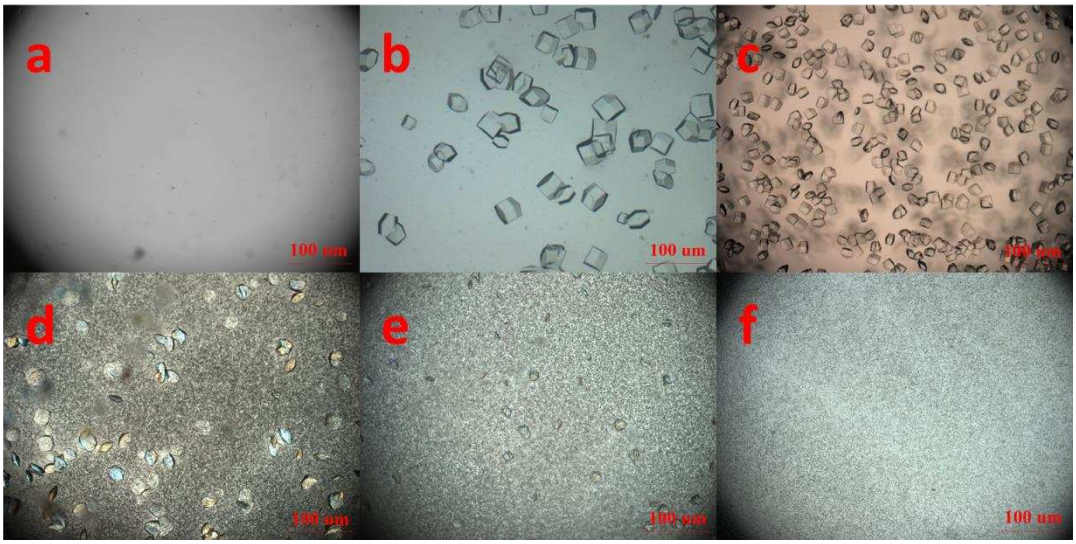

Figure 3: The microscope images of crystals obtained from the crystallization in quartz crucible, in which the temperature was decreased from 20 ℃ to 0 ℃ at different constant cooling rates: (a) before the cooling was started; (b) 0.03 ℃ min^{-1}; (c) 0.2 ℃ min^{-1}; (d) 0.3 ℃ min^{-1}; (e) 0.6 ℃ min^{-1}; and (f) 1.0 ℃ min^{-1}.

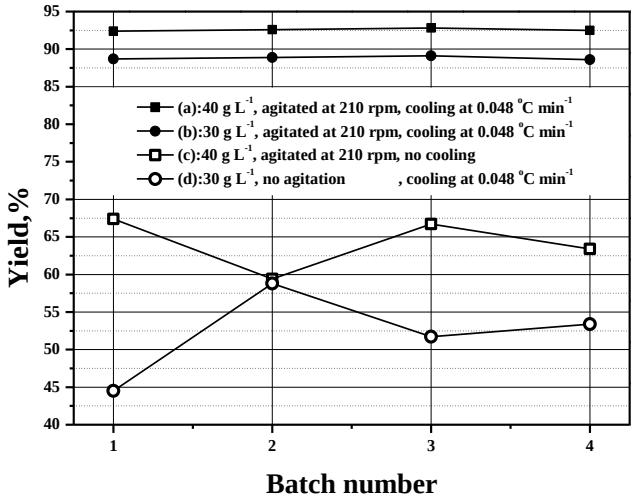

Figure 4: The yields obtained within 417 min of the crystallization in 5-mL crystallizer using 10% (w/w) NaCl, 0.1 M sodium acetate buffer, pH 4.5 and different conditions.

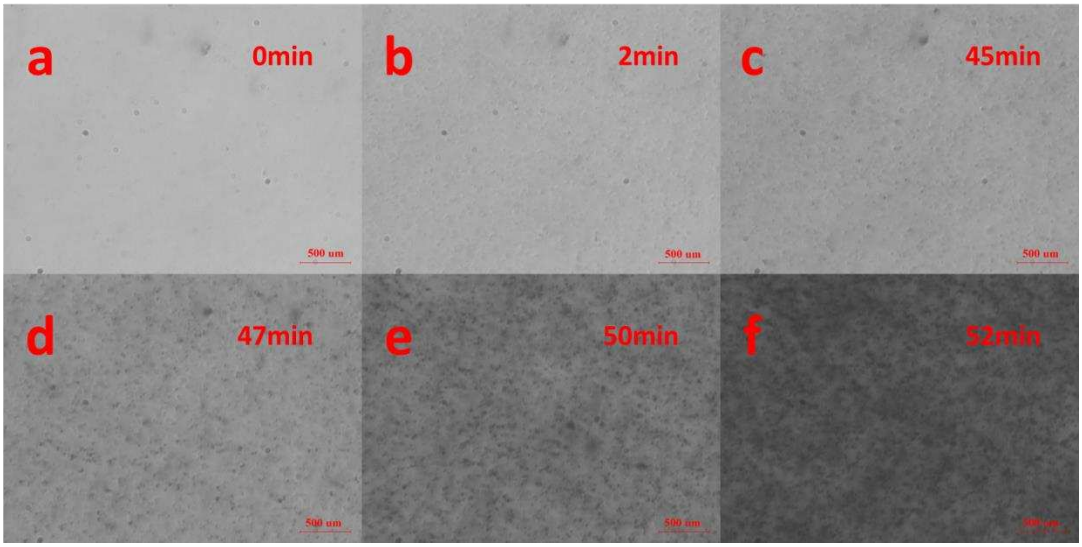

Figure 5: The online images of crystals grown from 40 g L^{-1} lysozyme and 10% NaCl with cooling from 20 to 0 °C at 0.048 °C min^{-1} in a 5-ml crystallizer, agitated at 210 rpm. The images were taken at different time intervals: a-b, fine particles; b-c, slowly grown fine particles; c-d, rapidly grew grown particles; and d-f, further grown particles with sharply increased solid concentration.

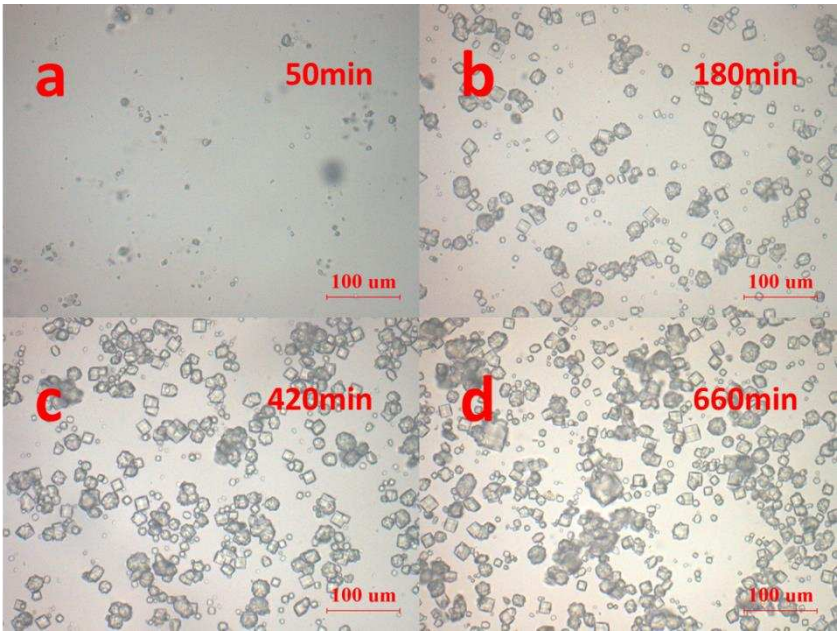

Figure 6: The microscopic images of crystals grown from 40 g L^{-1} lysozyme and 10% NaCl with cooling from 20 to 0 °C at 0.048 °C min^{-1} in a 5-ml crystallizer agitated at 210 rpm. The images were taken at different time: (a) 50 min; (b) 180 min; (c) 420 min; and (d) 660 min.

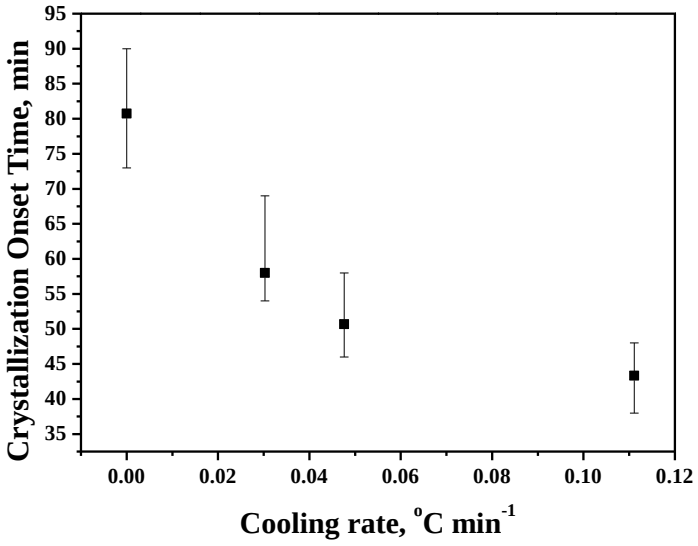

Figure 7: The crystallization onset time (determined from the online images) of solution containing 40 g L^{-1} lysozyme, 10% (w/w) NaCl and 0.1 M sodium acetate buffer, pH 4.5 as a function of cooling rate. The crystallization was carried out in a 5-ml crystallizer agitated at 210 rpm.

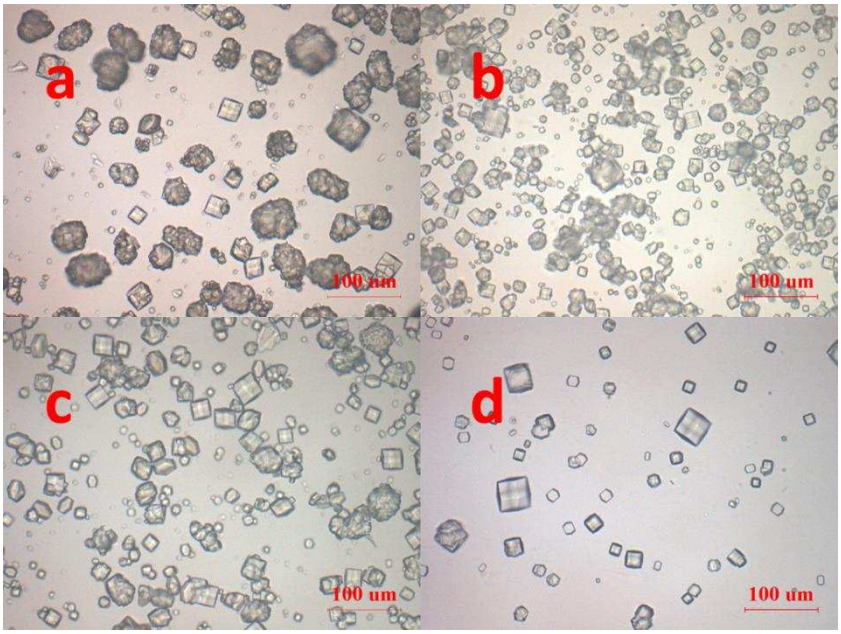

Figure 8: The microscopic images of lysozyme crystals (at 660 min) obtained at different cooling rates: (a) 0.111 °C min^{-1}; (b) 0.048 °C min^{-1}; (c) 0.030 °C min^{-1}; and (d) 0 °C min^{-1}. The crystallization was conducted in a 5-ml crystallizer stirred at 210 rpm using a solution containing 40 g L^{-1} lysozyme, 10% (w/w) NaCl and 0.1 M sodium acetate buffer, pH 4.5.

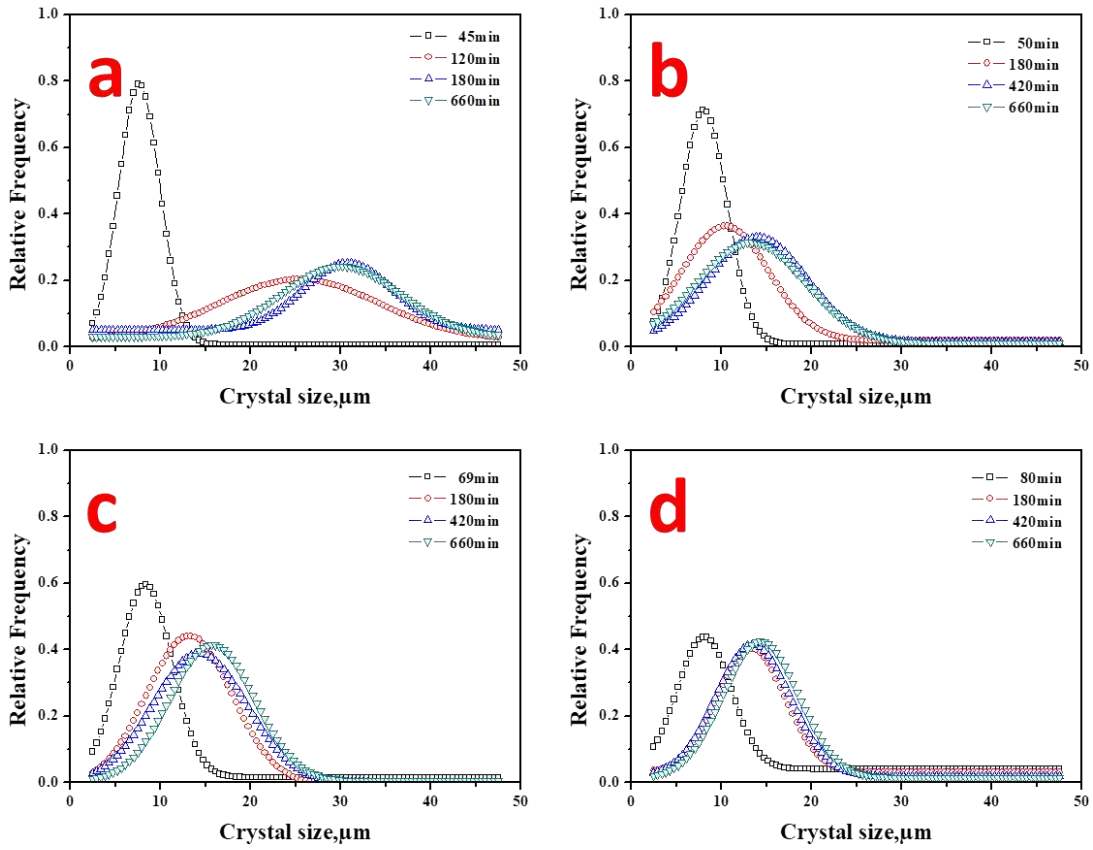

Figure 9: The crystal size distribution obtained at different cooling rates: (a) 0.111 °C min^{-1}; (b) 0.048 °C min^{-1}; (c) 0.030 °C min^{-1}; and (d) 0 °C min^{-1}. The crystallization was carried out in a 5-ml crystallizer, stirred at 210 rpm from using a solution containing 40 g L^{-1} lysozyme, 10% (w/w) NaCl and 0.1 M sodium acetate buffer, pH 4.5.

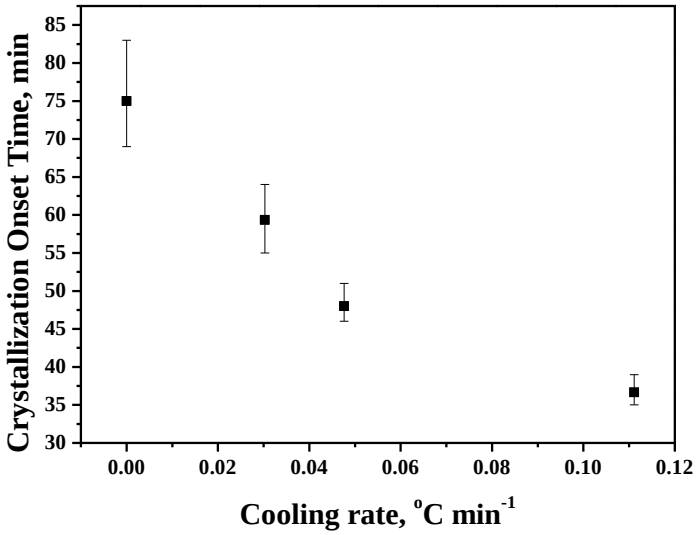

Figure 10: The crystallization onset time (obtained from online images) as a function of cooling rate. The crystallization was conducted in a 100-ml crystallizer, stirred at 210 rpm using a solution

containing 40 g L^{-1} lysozyme, 10% (w/w) NaCl and 0.1 M sodium acetate buffer, pH 4.5.

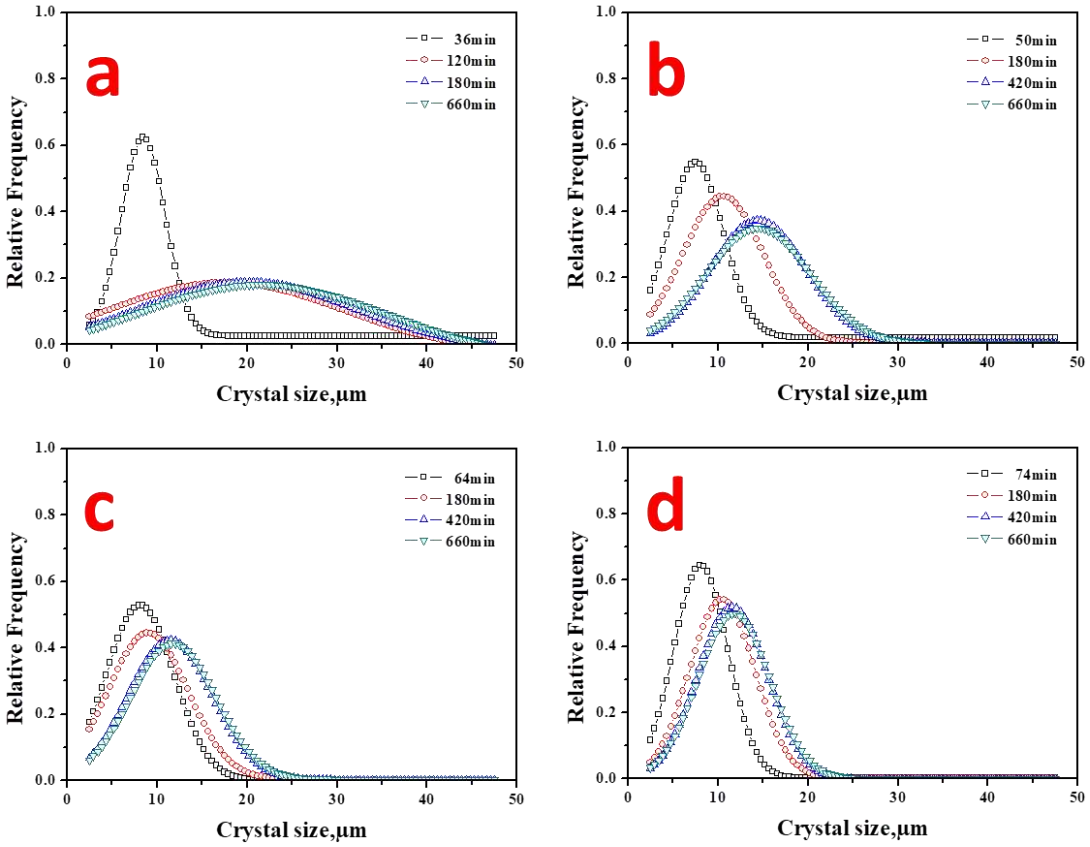

Figure 11: The crystal size distribution obtained at different cooling rates: (a) 0.111 °C min^{-1}; (b) 0.048 °C min^{-1}; (c) 0.030 °C min^{-1}; and (d) 0 °C min^{-1}. The crystallization was carried out in a 100-ml tank, stirred at 210 rpm using a solution containing 40 g L^{-1} lysozyme, 10% (w/w) NaCl and 0.1 M sodium acetate buffer, pH 4.5.

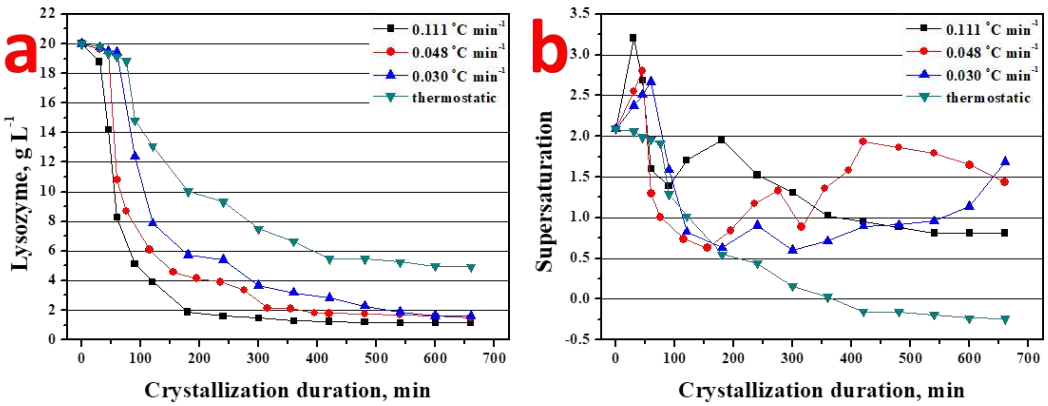

Figure 12: Lysozyme concentration profiles (after mixing with precipitant) (a) and supersaturation profiles (b) obtained from the crystallization at different cooling rates in a 100-ml crystallizer. Squares, 0.111 °C min^{-1}; Circles, 0.048 °C min^{-1}; Triangle, 0.030 °C min^{-1}; and Inverted triangle, 0 °C min^{-1}.

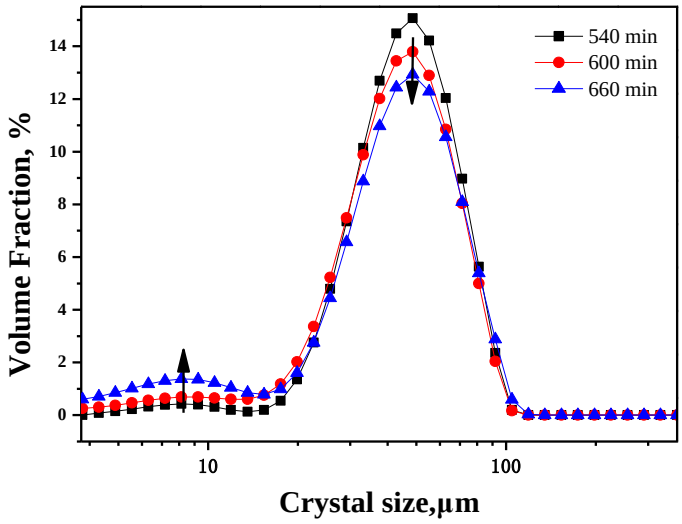

Figure 13: The size distributions of lysozyme crystals obtained at different crystallization durations: squares, 540 min; circles, 600 min; and triangle, 660 min. The crystallization was conducted in a 1-L crystallizer, stirred at 210 rpm using a solution containing 40 g L^{-1} lysozyme, 10% (w/w) NaCl and 0.1 M sodium acetate buffer, pH 4.5.